Conf-941270--1

UCRL-JC-119217
PREPRINT

Superplastic Ceramics and Intermetallics and Their Potential Applications

J. Wadsworth
T. G. Nieh

This paper was prepared for submittal to the
Superplasticity–60 Years after Pearson Conference
Manchester, United Kingdom
December 7–8, 1994

November 1994

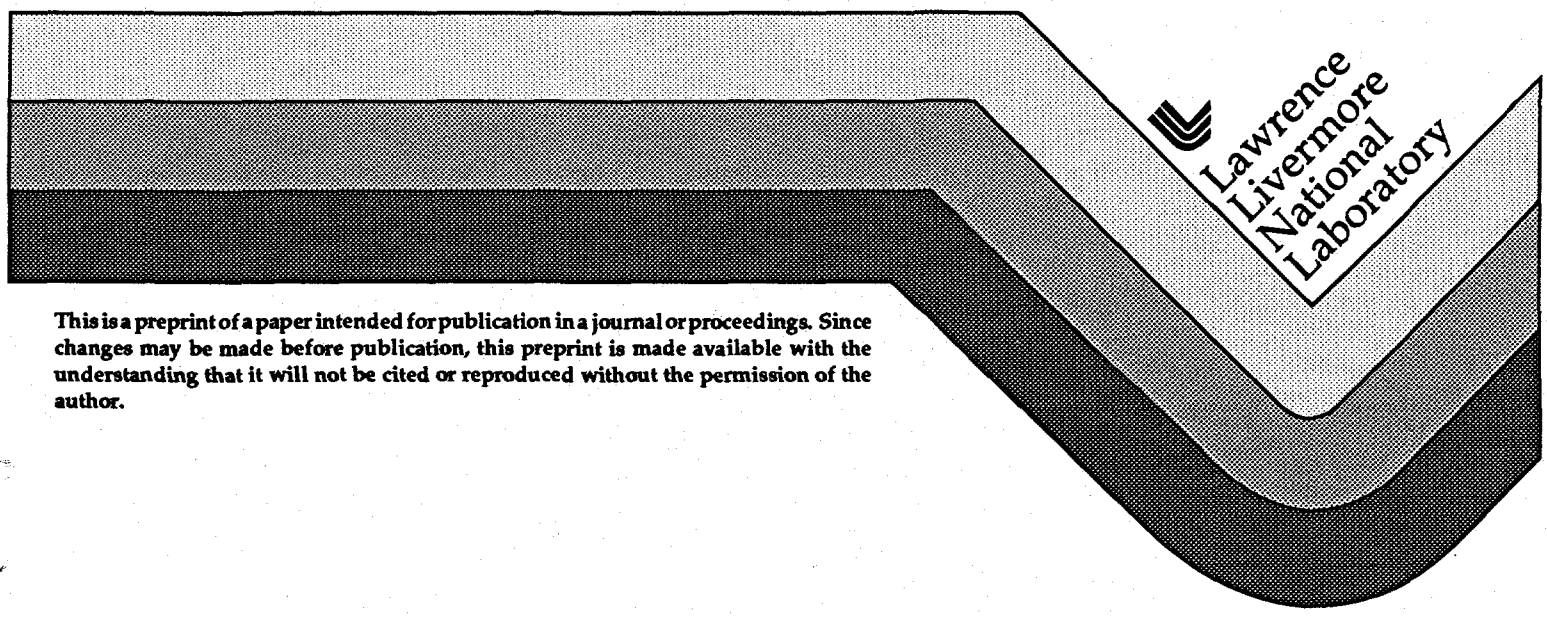

SUPERPLASTIC CERAMICS AND INTERMETALLICS AND THEIR POTENTIAL APPLICATIONS

J. Wadsworth and T.G. Nieh

Lawrence Livermore National Laboratory
P.O. Box 808, L-353, Livermore, CA 94550

Abstract

Recent advances in the basic understanding of superplasticity and superplastic forming of ceramics and intermetallics are reviewed. Fine-grained superplastic ceramics, including yttria-stabilized tetragonal zirconia polycrystal, Y– or MgO–doped Al_2O_3, Hydroxyapatite, β-spodumene glass ceramics, Al_2O_3–YTZP two-phase composites, SiC–Si_3N_4, and Fe–Fe_3C composites, are discussed. Superplasticity in the nickel-base (e.g., Ni_3Al and Ni_3Si) and titanium-base intermetallics (TiAl and Ti_3Al), is described. Deformation mechanisms as well as microstructural requirements and effects such as grain size, grain growth, and grain-boundary phases, on the superplastic deformation behavior are addressed. Factors that control the superplastic tensile elongation of ceramics are discussed. Superplastic forming, and particularly biaxial gas-pressure forming, of several ceramics and intermetallics are presented with comments on the likelihood of commercial application.

Superplastic Ceramics

The forming and shaping of ceramics are difficult because the melting points of ceramics are relatively high and, consequently, the temperatures required to thermally activate plastic deformation in ceramics are also high. In addition, the propensity for grain boundary separation in ceramics is well known. In the 1950s, extensive efforts were made in the western world to hot fabricate ceramics using conventional metallurgical processes such as extrusion, rolling, and forging [1,2]. The goal was to produce near-net-shape parts in order to avoid the expensive machining of ceramics. A number of structural oxides, including CaO, MgO, SiO_2, ZrO_2, BeO, ThO_2, and Al_2O_3, were studied. As a result of this work, an improved understanding of ceramic deformation was developed but certain problems, and in particular the requirement for relatively high forming temperatures, still existed. For example, the temperature required for hot forging Al_2O_3 was found to be about 1900°C which is extremely high from a practical standpoint. Subsequently, the concept of thermomechanical processing of ceramics was more or less abandoned.

The first observation of fine structure superplasticity in ceramics, in a yttria-stabilized tetragonal zirconia, is generally attributed to Wakai in 1986 [3], although an elongation to failure of ~100% in polycrystalline MgO was reported in 1965 by Day and Stokes [4]. Many other claims have been made of superplastic behavior in ceramics, but nearly all are based upon tests carried out only in compression [5-7]. It is important to point out that superplasticity refers to high ductility in tension and so enhanced plasticity data from compression tests cannot necessarily be considered to be convincing evidence of superplasticity. This is because ceramics often exhibit high values of strain rate sensitivity exponent (m is often equal to 1) in compression tests, but nonetheless show very limited tensile ductility. Tensile ductility at elevated temperatures is limited primarily by grain boundary cavitation which is initiated by tensile stresses but usually suppressed by compressive stresses. Since 1986, a number of fine-grained polycrystalline ceramics have been demonstrated to be superplastic in tension. These include yttria-stabilized tetragonal zirconia polycrystal (YTZP) [3,8], Y_2O_3- or MgO-doped Al_2O_3 [9], Hydroxyapatite [10], β-spodumene glass ceramics [11], Al_2O_3-reinforced YTZP (Al_2O_3-YTZP) [12,13], SiC-reinforced Si_3N_4 (SiC-Si_3N_4) [14,15], and iron-iron carbide (Fe-Fe_3C) [16] composites. The area of superplastic ceramics has been the subject of considerable interest and some review papers are now available [17,18].

Mechanical Properties

A summary of the microstructure and properties of some of the superplastic ceramics and ceramic composites are listed in Table 1. Generally, superplastic flow in ceramics is a diffusion-controlled process and the strain rate, $\dot{\varepsilon}$, can be expressed as

$$\dot{\varepsilon} = A \cdot d^{-p} \cdot \sigma^{n} \cdot exp(-\frac{Q}{RT}) \qquad \text{Equ. 1}$$

where d is the grain size, σ is the flow stress, Q is the activation energy for flow, R is the gas constant, T is the absolute temperature and A, p, and n are constants. The values for p, n, and Q vary according to the microstructure, the specific flow/diffusion law, and sometimes the impurity content in a material.

Table 1 Data for Superplastic Ceramics and Ceramic Composites in Tension

Material	Microstructure	Testing Parameters	Max. Elong., %	Material Variables*	Ref.
Monolithics					
3YTZP	d = 0.3 μm	450°C 5×10^{-4} s^{-1}	120	n = 2, p = 2, Q = 590 kJ/mol	[3]
3YTZP	d = 0.30 μm no glassy phase	1550°C 8.3×10^{-5} s^{-1}	800	n = 1.5, p = 3, Q = 510 kJ/mol	[19]
3YTZP	d = 0.3 μm	1450°C 4.8×10^{-5} s^{-1}	246	n = 2, p = NA, Q = 580 kJ/mol	[20]
Al_2O_3-500 ppm Y_2O_3	d = 0.66 μm	1450°C ~ 10^{-4} s^{-1}	> 65	n = NA, p/n = 1.5, Q = NA	[9]
Hydroxyapatite	d = 0.64 μm	1050°C 1.4×10^{-4} s^{-1}	> 150	n > 3, p/n = 1, Q = NA	[10]
β-spodumene glass	d = 0.91-2.0 μm >4 vol% glassy phase	1200°C 10^{-4} s^{-1}	> 400	n = 1, p = 3.1, Q = 707 kJ/mol	[11]
Composites					
20wt% Al_2O_3/YTZP	d = 0.50 μm no glassy phase	1650°C 4×10^{-4} s^{-1}	620	n = 2, p = 1.5, Q = 380 kJ/mol	[13]
20wt% Al_2O_3/YTZP	d = 0.50 μm	1450°C 10^{-4} s^{-1}	200	n = 2, p = NA, Q = 600 kJ/mol	[12]
10 vol% ZrO_2/Al_2O_3	d = 0.5 μm	1400°C 10^{-4} s^{-1}	>100	n = ?, p = ?, Q = ?	[21]
20wt% YTZP/Al_2O_3	d (ZrO_2) = 0.47 μm d (Al_2O_3) = 1.0 μm	1550°C 2.8×10^{-4} s^{-1}	110	n = 2, p = NA, Q = 700 kJ/mol	[22]
30wt% TiC/Al_2O_3	d = 1.2 μm	1550°C 1.2×10^{-4} s^{-1}	66	n = 4, p = NA, Q = 853 kJ/mol	[23]
β′-SiAlON	d = 0.4 μm with glassy phase	1550°C 10^{-4} s^{-1}	230	n = 1.5, p = NA, Q = NA	[24]
20 wt% SiC/Si_3N_4	d = 0.2-0.5 μm with glassy phase	1600°C 4×10^{-5} s^{-1}	>150	n = 2, p = NA, Q = 649-698 kJ/mol	[25]
20 vol% Fe/Fe_3C	d = 3.4 μm	1000°C 10^{-4} s^{-1}	600	n = 1.6, p = 2.9, Q = 200-240 kJ/mol	[16]

The specific functional relationship among the material variables are dependent upon the material, and strain rate and temperature ranges. The n value is noted in Table 1 to be less than 2 for all materials, except for hydroxyapatite. Also, superplastic flow in these materials is noted to be dependent upon grain size. The grain size exponent, p, ranges from 1 to 3, which is within the range of various diffusion controlled flow models. Grain sizes in all the superplastic ceramics with tensile elongation greater than 100% except for Fe/Fe_3C, are noted to be less than 1 μm, which is much

smaller than the grain size found in superplastic metals (typically, ~10 μm). Because of the fineness of the microstructure, grain growth, and in particular dynamic grain growth, usually occurs during superplastic deformation of ceramics [26-28]. Grain growth normally follows a mathematical expression of the form [26,29]

$$D^{\ell} - D_o^{\ell} = kt \qquad \text{Equ. 2}$$

in which $\ell \sim 3$, and D and D_o represent the instantaneous and initial grain sizes, respectively, k is a kinetic constant which depends primarily on temperature and grain boundary energy, and t is the time. Since the tensile ductility of superplastic ceramics decreases with increasing grain size, dynamic grain growth deteriorates the properties of superplastic ceramics. In addition, dynamic grain growth can affect the accurate value of strain rate sensitivity. For example, the reported strain rate sensitivity exponent values for superplastic YTZP vary from 0.3 [8,30,31] to 0.5 [3,20,27,32], in part, resulting from microstructural evolution during deformation [33]. For example, Nieh and Wadsworth [33] have determined the true m value to be about 0.67 (i.e., one measured under constant structure conditions), by normalizing the stress with the square of the final grain size; this result is illustrated in Fig. 1.

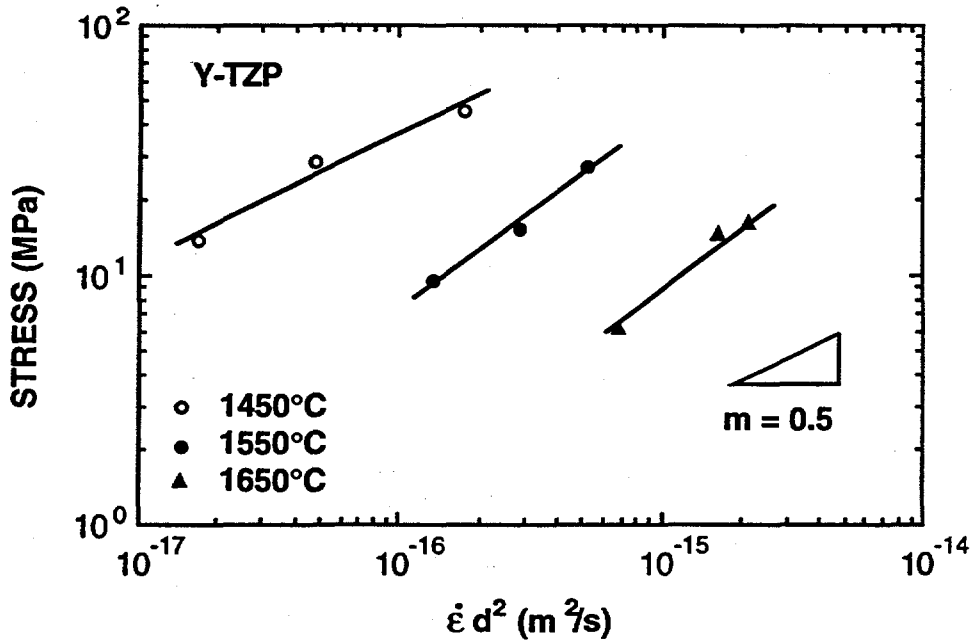

Fig. 1 Flow stress as a function of grain size normalized strain rate. The strain rate sensitivity exponents are less than 0.5 at all temperatures. (from Ref. [33])

In contrast to metals, ceramics generally exhibit high values of m, the tensile ductility of ceramics is nonetheless limited, indicating that necking stability does not govern the tensile ductility of ceramics. Kim *et al.* [34] and Chen and Xue [17] independently found that flow stress plays a dominant role in determining the tensile elongation of superplastic ceramics. Plotted in Fig. 2 is the true fracture strain of many superplastic ceramics as a function of flow stress; the true fracture strain is a linearly decreasing function of the logarithm of the flow stress. This result is directly related to the fact that when the flow stress is lower than the grain boundary strength of the material, intergranular failures do not occur and the material deforms plastically. As the flow stress is increased, so is the likelihood that the cohesive strength of grain boundaries will be reached. Once this level of stress is attained, intergranular cavitation and cracking occur, and the elongation to failure is decreased.

To illustrate the reverse effect of strengthening on ductility, Dougherty *et al.* [35] recently performed experiments with Al_2O_3 particle and SiC whisker reinforced fine-grained YTZP. Experimental results showed that the addition of SiC whiskers to YTZP causes a significant strengthening effect, but not for the Al_2O_3 particle reinforced composite. As shown in Fig. 3, at 1550°C and a strain rate of $10^{-3}\,s^{-1}$, the flow stresses of both YTZP and a 20 wt% (28 vol%) Al_2O_3 particle-reinforced YTZP are both less than 30 MPa, whereas the flow stress of 20 vol% SiC whisker

reinforced YTZP is almost 200 MPa. All of the three materials have a fine-grained matrix (~0.5 μm). As a result of the strengthening effect, the maximum elongation value of the SiC/YTZP composite was only 50%. In contrast, both the YTZP and Al_2O_3 particle reinforced YTZP composite behave superplastically.

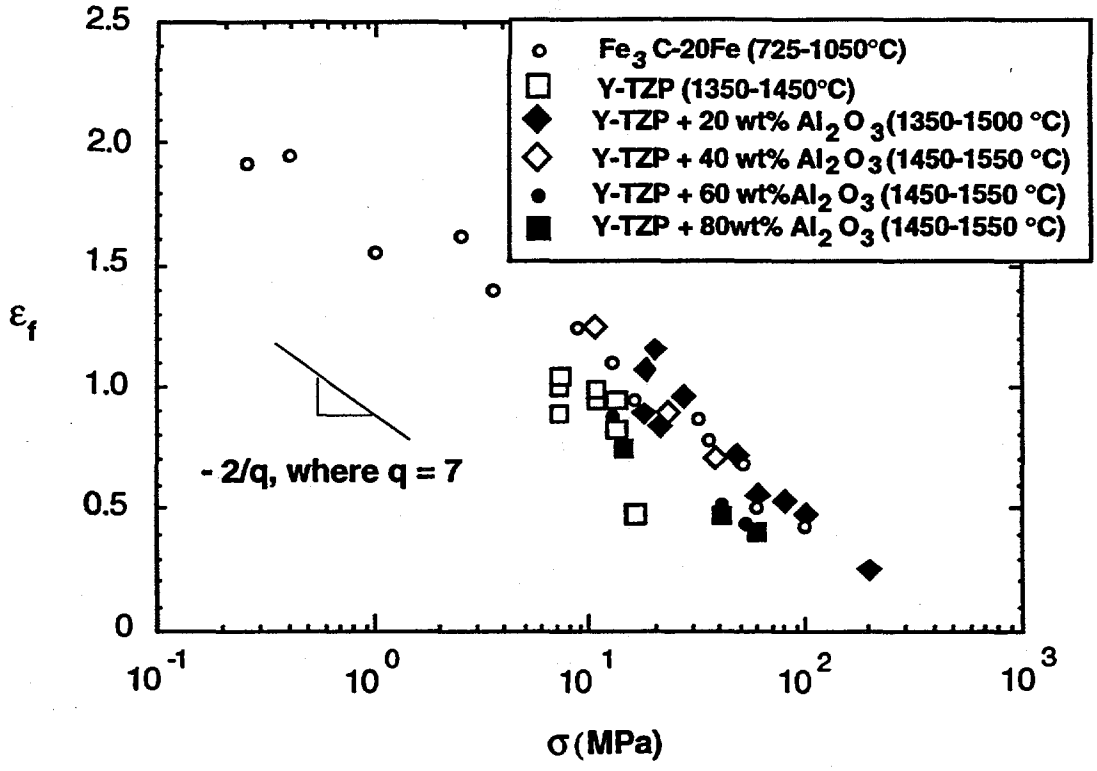

Fig. 2 Fracture strain as a function of the logarithm of the flow stress for superplastic iron carbide and YTZP based ceramics. (from Ref. [34])

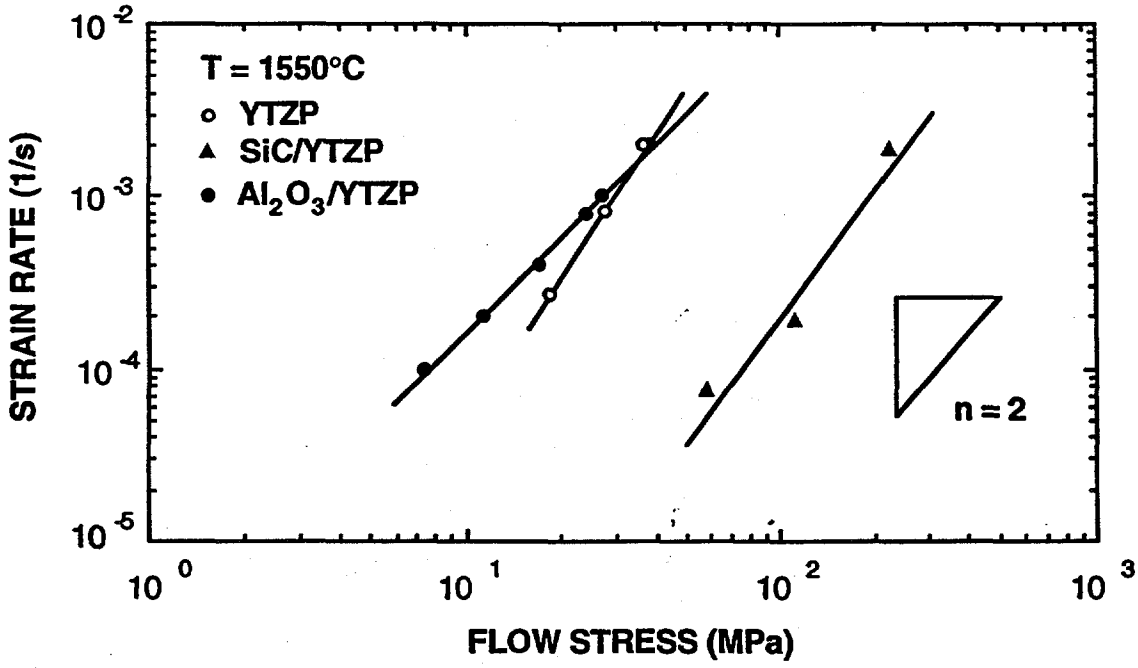

Fig. 3 Direct comparison of the strengths of YTZP and SiC/YTZP and Al_2O_3/YTZP composites at 1550°C. (from Ref. [35])

Grain-Boundary Structure

A general question concerning the microstructure of superplastic ceramics is: "Is the presence of a grain-boundary glassy phase necessary in order to produce superplasticity?" Nieh *et al.* [36] have presented several pieces of experimental evidence to show that there is no grain boundary glassy phase in their superplastic YTZP and 20 wt%Al_2O_3/YTZP samples. These experimental results include high resolution lattice images of grain boundary triple junctions in YTZP, shown in Fig. 4(left), in which lattice fringes from adjoining grains can be followed to their intersections at both the grain boundary interface and the triple junction. In addition, X-ray photoelectron Spectroscopy (XPS) from the intergranular fracture surfaces of superplastically deformed specimens, shown in Fig. 4(right), indicate the absence of low melting point glassy phases in YTZP and 20 wt%Al_2O_3/YTZP. These results suggest that the presence of a grain boundary glassy phase is unnecessary for superplasticity in fine-grained ceramics. Although the presence of a liquid phase at grain boundaries may not be a necessary prerequisite for superplasticity in ceramics, its presence can definitely affect some of the kinetic processes, such as grain boundary sliding. For example, Wakai *et al.* [37] and Chen and co-workers [17,38] have both demonstrated that the presence of grain-boundary glassy phases can, in general, reduce the superplastic forming temperatures for various ceramics, including YTZP and Si_3N_4.

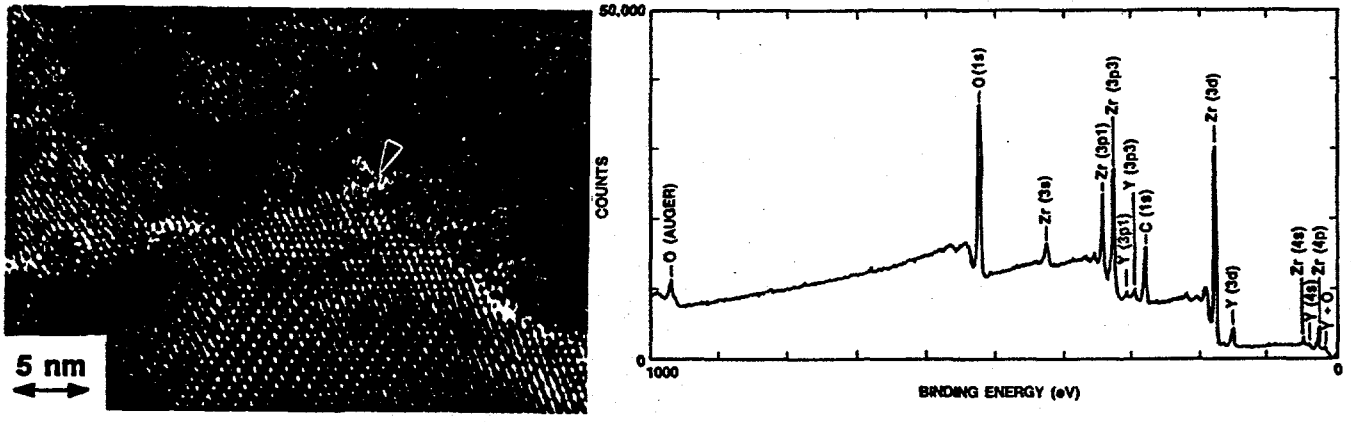

Fig. 4 (left) High resolution lattice image of a grain boundary triple junction in fine-grained superplastic YTZP, and (right) XPS spectrum from the fracture surface of a superplastic YTZP sample, indicating the absence of any second phase. (from Ref. [36])

Superplastic Intermetallics

Although large tensile elongations (~100%) for an intermetallic (Sendust, Fe-9.6wt%Si-5.4wt%Al) were indicated as early as 1981 [39], the observation of true superplastic intermetallics was not reported until 1987 [40]. Up to the present time, several intermetallics of the $L1_2$ structure (e.g., Ni_3Al [40-42] and Ni_3Si [43,44]), Fe_3Al [45], titanium aluminide (TiAl [46-48]), and trititanium aluminides (Ti_3Al [49,50]), have been demonstrated to be superplastic. Similar to the case for superplastic metals, superplasticity in intermetallics has been recorded in both quasi-single-phase and two-phase materials. The strain rate sensitivity ranges typically from 0.3 to 1. One interesting observation is that some intermetallics exhibit superplastic properties, even in the relatively coarse-grained (>10 μm) conditions [39,43,45].

Nickel-base

Two Ni-base intermetallics, Ni_3Si and Ni_3Al, have been demonstrated to be superplastic. A summary of the superplastic properties of Ni-base intermetallics is listed in Table 2. It is noted that the superplastic deformation of Ni_3Si and Ni_3Al can be well described by a classical equation (Equ. 1). The exact values for n, p, Q, and the material constant A in Equ. 1 for each material, of course, are determined by the temperature and strain rate regions in which superplastic properties of the material are characterized.

Table 2 Property data of superplastic Ni-base intermetallics

composition (wt%)	d, (μm)	T, (°C)	$\dot{\varepsilon}$, (s^{-1})	m	el. (%)	Ref.
Ni-9%Si-3.1%V-2%Mo (duplex)	15	1080	8×10^{-3}	0.5	710	[43]
Ni-9%Si-3.1%V-4%Mo (duplex)	>10	1070	10^{-3}	0.43	560	[43,51]
Ni_3(Si,Ti) (single-phase)	4	850	6×10^{-5}	0.43	180	[44]
0.24 at% B-doped Ni_3Al (single-phase)	1.6	700	5×10^{-5}	0.42	160	[41]
Ni-8.5%Al-7.8%Cr-0.8%Zr-0.02%B (duplex)	6	1100	8.3×10^{-4}	0.75	640	[42]

In the case of duplex Ni_3Si alloy, superplasticity was observed over a limited temperature range from 1000 to 1100°C, but over a wide strain rate range from 6×10^{-4} to 1 s^{-1}. A tensile elongation of over 200% can be generally obtained under all the above test conditions, and a maximum elongation to failure of 710% has been recorded at 1080°C at a strain rate of 8.0×10^{-3} s^{-1}. Strain rate as a function of flow stress is plotted in Fig. 5. The strain rate sensitivity, m, is determined to be about 0.5, which is a typical value in many superplastic metals, at a strain rate $> 4 \times 10^{-3}$ s^{-1}. In the low strain rate region, the m value increases and approaches one, probably resulting from the fact that the testing temperatures are over 0.9 T_m. This near-Newtonian-viscous behavior indicates that the deformation mechanism either changes from grain boundary sliding to a diffusion-type mechanism, such as Coble Creep or Nabarro-Herring Creep, or it may be a result of slip accommodation by a dislocation-glide mechanism [52]. The activation energy for the m = 0.5 region is calculated to be about 555 kJ/mol which is relatively high in comparison to the value of activation energy for superplastic deformation measured in a fine-grained nickel base superalloy MA754 of 267 kJ/mol [53]. In another study, Takasugi *et al.* [54] processed single-phase Ni_3(Si,Ti) into a fine-grained condition (~4 μm) and characterized the superplastic behavior of the alloys. The fine-grained material exhibits superplasticity (elongation = 180%) at temperatures between 800 and 900°C and at strain rates between 6.0×10^{-5} and 10^{-3} s^{-1}. These deformation temperatures are only about 0.8 T_m, where T_m is the absolute melting point of Ni_3(Si,Ti), whereas superplasticity is found at about 0.85-0.94 T_m for duplex Ni_3Si alloys. This is primarily attributed to the fact that grains in the single-phase Ni_3Si coarsen quickly at T > 850°C, while the microstructures of the duplex alloys are more thermally stable.

In the case of Ni_3Al, superplasticity has been produced in both single-phase [41] and duplex [42] alloys, and in both powder-metallurgy [40,42] and ingot-metallurgy [41] products. In the case of PM alloys, the superplastic IC-218 (composition of Ni-18 at%Al-8 at%Cr-1 at%Zr-0.15 at%B) had a duplex microstructure, containing about 10 to 15% of disordered γ phase in an ordered γ' phase matrix, and a grain size of about 6 μm. The alloy exhibited superplasticity (maximum elongation = 640%) at temperatures from 950 to 1100°C and strain rates from 10^{-5} to 10^{-2} s^{-1}. At strain rates $> 7 \times 10^{-2}$ s^{-1}, the strain rate sensitivity value is about 0.32. It increases to 0.75 over the strain rate range from 7×10^{-2} to 4×10^{-4} s^{-1} below which the m value appears to increase to an even higher value (i.e., it approaches 1). Single-phase, boron-doped (0.24 at.%) Ni_3Al has been reported to be superplastic [41]. The material is of ultrafine grain size (~1.6 μm). A maximum elongation of 160% was recorded at 700°C and at a strain rate of less than 10^{-4} s^{-1}. Superplasticity in this single-phase Ni_3Al takes place via dynamic recrystallization. Although the single-phase Ni_3Al has a finer grain size than the duplex Ni_3Al (1.6 μm vs 6 μm), superplastic elongation of the single-phase alloy is much inferior to that of the duplex alloy. A lower superplastic elongation in the single-phase Ni_3Al is believed, in part, to be related to the less stable grain structure under high temperature and dynamic conditions.

One of the interesting characteristics of the superplastic duplex Ni_3Si is that the temperature range is quite limited, ranging only from about 1000 to 1100°C; Ni_3Si is single-phase below 1000°C. However, superplasticity can exist over a relatively wide strain rate range. For example, at 1080°C, a

change in strain rate over three orders of magnitude, from 10^{-3} to 1 s^{-1}, only results in a decrease in tensile elongation from 650 to 300%. An elongation value of 300% is still considered to be superplastic, and a strain rate of 1 s^{-1} is considered to be very high; in fact, such a strain rate is within the range for conventional forging. This offers a technological benefit of superplastic forming of Ni_3Si at high strain rates. In contrast to duplex Ni_3Si, the superplastic strain of duplex Ni_3Al depends strongly on the strain rate. For example, the tensile elongation of Ni_3Al reduces from 440% to only 100% when the strain rate increases by one order of magnitude (from 8×10^{-4} to 8×10^{-3} s^{-1}) at 1050°C [42].

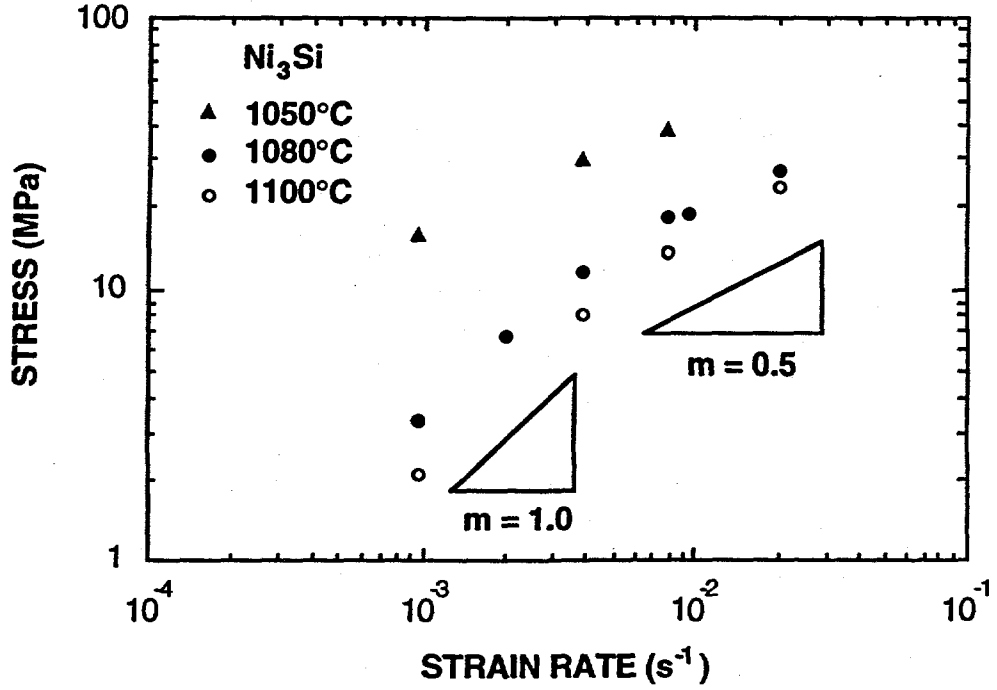

Fig. 5 Strain rate as a function of flow stress for superplastic duplex Ni_3Si. The stress exponent, m, is approximately 0.5 and approaches one in the high strain rate region. (from Ref. [43])

Titanium-base

Superplasticity has been observed in both TiAl (γ) and Ti_3Al (α_2). In the case of Ti_3Al, only duplex alloys, Ti-25Al-10Nb-3V-1Mo (super α_2) [50] and Ti-24Al-11Nb (α_2) [50,55] have been shown to be superplastic. These alloys were thermomechanically processed to fine-grained (about 5 μm) conditions. Superplasticity exists in a narrow temperature range (950 to 1020°C); within this temperature range the volume fraction of β phase is about 0.4-0.6 [55]. Maximum tensile elongation values of about 500% and 1350% were recorded in the α_2 and super α_2 alloys, respectively, at a strain rate of approximately 10^{-5} s^{-1}. The measured strain rate sensitivity values of both alloys are above 0.5, and it is believed that a grain boundary sliding mechanism is responsible for the observed superplasticity. It was particularly pointed out by Ridley *et al.* [55] that super α_2 remained free from cavitation after large superplastic tensile elongation (>1000%). This suggests the alloy is suitable for stretch forming without the need to impose back pressure to inhibit cavitation.

Studies of superplastic TiAl are of the most recent origin. A summary of published work on superplastic TiAl is listed in Table 3. All materials, except PM Ti-47Al, were produced by ingot casting techniques. As shown in Table 3, superplasticity is only observed in fine-grained, two-phase ($\gamma+\alpha_2$) TiAl alloys, with the exception of the Ti-43Al-13V alloy which is ($\gamma+\beta$). The fine microstructure is achieved if a composition is selected in the two-phase region where approximately 50 vol% of each of the two aluminides, TiAl and Ti_3Al, coexist [46].

Table 3 Property data of superplastic TiAl

composition (at%)	d, (μm)	T, (°C)	$\dot{\varepsilon}$, (s^{-1})	m	el. (%)	Ref.
Ti-43Al	5	1000–1100	10^{-5}–$2x10^{-2}$	0.5	275	[46]
Ti-50Al	<5	900–1050	$2x10^{-4}$–$8.3x10^{-3}$	~0.4	250	[56]
Ti-47Al-2Nb-1.6Cr-0.5Si-0.4Mn	20	1180–1310	$2x10^{-5}$–$2x10^{-3}$	0.65	470	[48]
Ti-47.4Al	8	927	10^{-4}	NA	~400	[47]
Ti-43Al-13V	NA	800-1143	3×10^{-4}–10^{-1}	NA	580	[57]
PM Ti-47Al	2	950	10^{-4}-10^{-3}	0.3	NA	[58]

A typical strain rate-flow stress curve for the fine-grained, equiaxed TiAl is presented in Fig. 6. The curves divide into two different stress exponent regions as a function of the flow stress. At high values of the flow stress, m = 0.25 is found. In this region, the rate-controlling deformation mechanism was suggested to be a diffusion-controlled dislocation process. At low values of the flow stress, m = 0.5 is observed at all temperatures. At the highest temperature of testing, 1100°C, the m = 0.5 region extends to a strain rate of as high as 10^{-3} s^{-1}. In this region, the material is superplastic and the rate-controlling deformation process is attributed to a grain boundary sliding mechanism. An elongation-to-failure value of only 275% was obtained at a strain rate of 2.5×10^{-4} s^{-1} at 1050°C, suffering the sample from oxidation during testing in air. (A higher maximum elongation of 470% has been recorded from a two-phase, relatively coarse-grained (~20 μm) TiAl tested in vacuum (3×10^{-3} Pa) [48]). The apparent activation energy, in the m = 0.5 region, was determined to be equal to 390 kJ/mole which is close to that measured from the creep of a fine-grained Ti(53 at.%)-Al(47 at.%) [59].

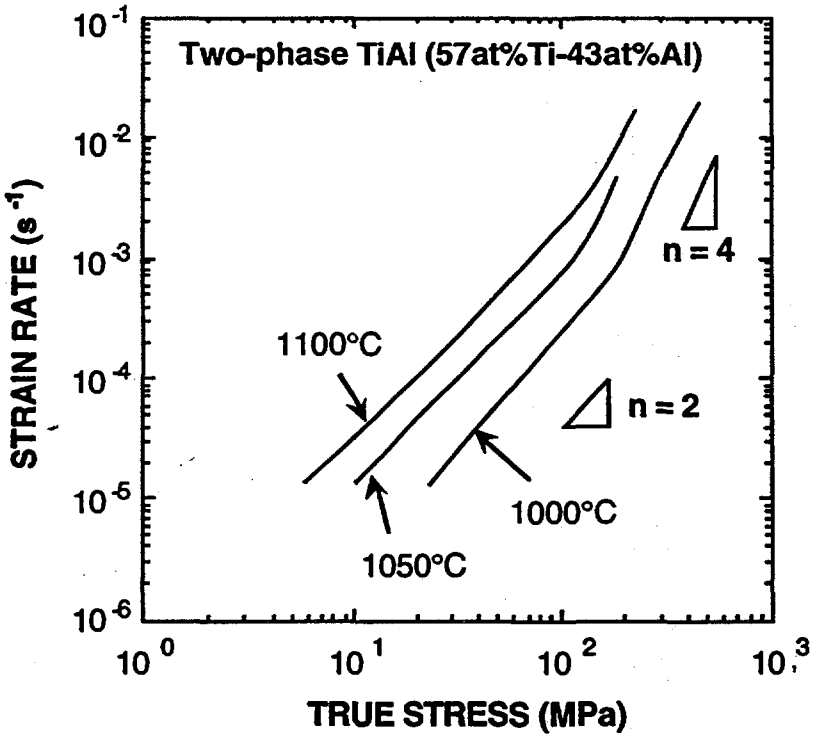

Fig. 6 Strain rate as function of flow stress for fine-grained, two-phase equiaxed TiAl. (data from Ref. [46])

Superplastic Forming of Ceramics

Improved understanding of superplastic ceramics has now advanced to the stage that technological application of ceramic superplastic deformation is receiving increasing attention. Examples of

superplastic forming include the extrusion of YTZP powders [29], closed die deformation of YTZP [60], punch forming of YTZP sheet [61] and biaxial gas-pressure deformation of 20%Al_2O_3/YTZP and YTZP [62,63] . In the case of gas-pressure deformation, the key features of the equipment are shown in Fig. 7. High-purity argon gas was used to impose the deformation pressure during forming operations. In-situ deformation is measured when the diaphragm expands upwards to form a hemisphere; this displaces a silicon carbide sensor rod linked to an LVDT. The forming pressure was monitored both with a dial indicator as well as with an electronic DC strain gauge pressure transducer. The apparatus was inductively heated and fully enclosed within a vacuum chamber. The typical heat-up time was 30 minutes with a ten minute stabilization time prior to the application of forming pressure. The apparatus is capable of forming ceramic discs of 50 mm diameter discs. The discs were clamped at their periphery resulting in an unconstrained diaphragm with a diameter of 38 mm, producing a hemisphere of 19 mm in height.

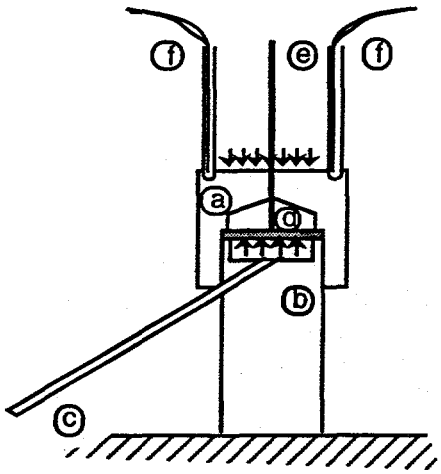

Fig. 7 Gas-pressure forming apparatus. Upper die (a) and lower die (b). Gas is admitted through integral pressure tube (c), ceramic diaphragm (d) deforms upwards causing movement of deflection sensor (e). Temperature is monitored by twin thermocouples (f).

Using the apparatus in Fig. 7, it is possible to make intricately shaped, net shaped parts from superplastic ceramic sheet. Examples of a cone-on-cylinder geometry, a hat section, and a hemisphere of YTZP are shown in Fig. 8. Various shape geometries are possible with this process – as determined by the shape of the die. Recently, Nieh and Wadsworth [64] also used the technology to successfully produce a sophisticated high temperature millimeter wave radome from Si wafers, as shown in Fig. 9. The radome was fabricated by co-deformation (superplastic forming/diffusion bonding) of a 10-cm-diameter silicon wafer with micromachined coolant slots and another silicon wafer. The structure in Fig. 9 would be extremely difficult, if not impossible, to make without using the gas-pressure forming process. In addition to Si, a hybrid YTZP/C103 (nominal composition: Nb-10Hf-1Ti.) ceramic-metal structure has been made using a superplastic forming/diffusion bonding technique [65]. Such a thin-walled engineered metal-ceramic structure could have great utility in high thermal flux applications. Other potential applications include manufacturing net shape turbine rotors directly from fine Si_3N_4 powders and the bulk forming of automotive components from superplastic Si_3N_4 [66].

Superplastic Forming of Intermetallics

There is only limited study on the superplastic forming of intermetallics. The aerospace application of titanium aluminides has not been widely revealed, although some demonstration parts has been made [67]. This is, in part, because of its proprietary or classified nature. Nonetheless, it is noted that super α_2 foils have been fabricated from sheet material by vacuum pack rolling in the temperature and strain rate ranges where the material is superplastic [68]. The foils can be used as facing sheet for further fabrication of intermetallic composites. Also noted is that, similar to that in the case of Si_3N_4, γ-TiAl are being actively evaluated to be used for turbine rotors and high-temperature gas valves [69]. As a result of the great difficulty in machining TiAl, net shape forming techniques would be attractive.

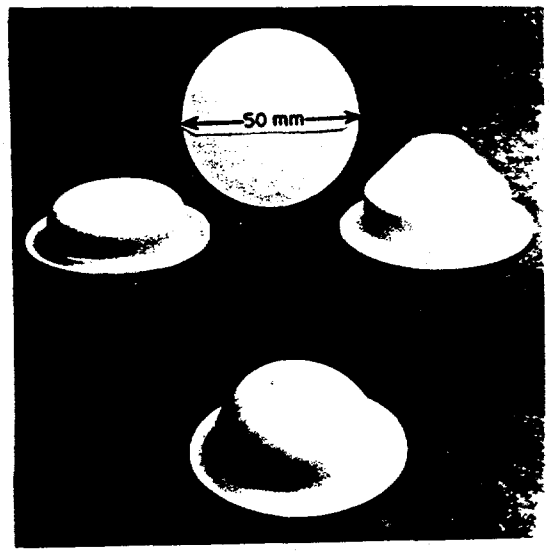

Fig. 8 Examples of a cone-on-cylinder geometry, a hat section, and a hemisphere superplastically-formed from YTZP and Al_2O_3/YTZP. (from Ref. [63])

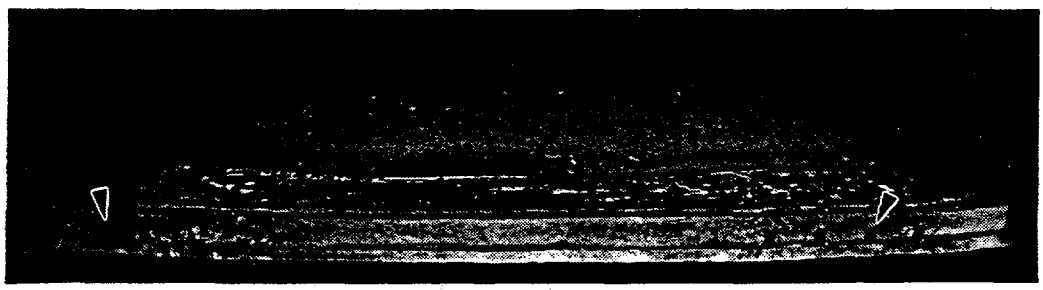

Fig. 9 High temperature millimeter wave Si radome manufactured by a concurrent superplastic forming and diffusion bonding technique. Cooling channels are indicated. (from Ref. [64])

Conclusions

Superplasticity has been observed in many fine-grained (< 1 μm) ceramics, including YTZP, Al_2O_3, hydroxyapatite, β-spodumene glass ceramics, and Al_2O_3-zirconia, SiC-Si_3N_4, and Fe_3C-Fe composites) as well as intermetallics, including Ni_3Al, Ni_3Si, Ti_3Al, and TiAl. In the case of ceramics, the presence of glassy phases may be unnecessary but can strongly affect the optimum temperature for superplasticity. The tensile elongation of a superplastic ceramic is found to be inversely proportional to the flow stress. In the case of intermetallics, two-phase alloys, despite having a relatively large grain size (>10 μm), exhibit better superplastic properties than single-phase alloys. For some alloys such as Ni_3Si, superplasticity appears to be relatively rate insensitive. Superplastic forming techniques have been demonstrated in some ceramics and intermetallics, but applications are primarily performance-driven (e.g., aerospace). High cost is still the major obstacle for wide-spread, commercial applications of superplastic ceramics and intermetallics.

Acknowledgment

This work was performed, in part, under the auspices of the U.S. Department of Energy by Lawrence Livermore National Laboratory under contract No. W-7405-Eng-48.

References

1. R.M. Fulrath, *Ceram. Bull.*, **43**, 880 (1964).

2. R.W. Rice, *Ultrafine-Grain Ceramics* (edited by J.J. Burke, N.L. Reed, and V. Weiss), p. 203, Syracuse University Press, Syracuse, NY (1970).
3. F. Wakai, S. Sakaguchi, and Y. Matsuno, *Adv. Ceram. Mater.*, **1**, 259 (1986).
4. R.B. Day and R.J. Stokes, *J. Am. Ceram. Soc.*, **49**, 345 (1966).
5. P.E.D. Morgan, "Superplasticity in Ceramics," in *Ultrafine-Grain Ceramics,* edited by J.J. Burke, N.L. Reed, and V. Weiss, Syracuse University Press, New York (1970), p. 251.
6. K.R. Venkatachari and R. Raj, *J. Am. Ceram. Soc.*, **69**, 135 (1986).
7. C.K. Yoon and I.W. Chen, *J. Amer. Ceram. Soc*, **73**, 1555 (1990).
8. T.G. Nieh, C.M. McNally, and J. Wadsworth, *Scr. Metall.*, **22**, 1297 (1988).
9. P. Gruffel, P. Carry, and A. Mocellin, *Science of Ceramics, Volume 14* (edited by D. Taylor), p. 587, The Institute of Ceramics, Shelton, Stoke-on-Trent, UK (1987).
10. F. Wakai, Y. Kodama, S. Sakaguchi, and T. Nonami, *J. Am. Ceram. Soc*, **73**, 257 (1990).
11. J.-G. Wang and R. Raj, *J. Am. Ceram. Soc.*, **67**, 399 (1984).
12. F. Wakai and H. Kato, *Adv. Ceram. Mater.*, **3**, 71 (1988).
13. T.G. Nieh and J. Wadsworth, *Acta Metall. Mater.*, **39**, 3037 (1991).
14. F. Wakai, *Superplasticity in Metals, Ceramics, and Intermetallics, MRS Proceeding No. 196R* (edited by M.J. Mayo, J. Wadsworth, and M. Kobayashi), p. 349, Materials Research Society, Pittsburgh, PA (1990).
15. T. Rouxel, F. Wakai, K. Izaki, and K. Niihara, *Pro. 1st Inter. Symp. on Science of Engineering Ceramics* (edited by S. Kimura and K. Niihara), p. 437, Ceramic Society of Japan, Tokyo. Japan (1991).
16. W.J. Kim, G. Frommeyer, O.A. Ruano, J.B. Wolfenstine, and O.D. Sherby, *Scr. Metall.*, **23**, 1515 (1989).
17. I.-W. Chen and L.A. Xue, *J. Am. Ceram. Soc.*, **73**, 2585 (1990).
18. T.G. Nieh, J. Wadsworth, and F. Wakai, *Inter. Mater. Rev.*, **36**, 146 (1991).
19. T.G. Nieh and J. Wadsworth, *Acta Metall. Mater.*, **38**, 1121 (1990).
20. T. Hermanson, K.P.D. Lagerlof, and G.L. Dunlop, *Superplasticity and Superplastic Forming* (edited by C.H. Hamilton and N.E. Paton), p. 631, TMS (1988).
21. L.A. Xue, X. Wu, and I.W. Chen, *J. Am. Ceram. Soc.*, **74**, 842 (1991).
22. F. Wakai, Y. Kodama, S. Sakaguchi, N. Murayama, H. Kato, and T. Nagano, *MRS Intl. Meeting on Advanced Materials Vol 7 (IMAM-7, Superplasticity)* (edited by M. Doyama, S. Somiya, and R.P.H. Chang), p. 259, Materials Research Soc., Pittsburgh, Pennsylvania (1989).
23. T. Nagano, H. Kato, and F. Wakai, *J. Am. Ceram. Soc.*, **74**, 2258 (1991).
24. X. Wu and I.-W. Chen, *J. Am. Ceram. Soc.*, **75**, 2733 (1992).
25. F. Wakai, Y. Kodama, S. Sakaguchi, N. Murayama, K. Izaki, and K. Niihara, *Nature (London)*, **334**, 421 (1990).
26. T.G. Nieh and J. Wadsworth, *J. Am. Ceram. Soc.*, **72**, 1469 (1989).
27. F. Wakai, S. Sakaguchi, and H. Kato, *J. Ceram. Soc. Japan (In Japanese)*, **94**, 72 (1986).
28. D.J. Schissler, A.H. Chokshi, T.G. Nieh, and J. Wadsworth, *Acta Metall. Mater.*, **39**, 3227 (1991).
29. B.J. Kellett, C. Carry, and A. Mocellin, *J. Amer. Ceram. Soc*, **74**, 1922 (1990).
30. C. Carry, *MRS Intl. Meeting on Advanced Materials Vol.7 (IMAM-7, Superplasticity)* (edited by M. Doyama, S. Somiya, and R.P.H. Chang), p. 251, Materials Research Soc., Pittsburgh, PA (1989).
31. Y. Ma and T.G. Langdon, *Superplasticity in Metals, Ceramics, and Intermetallics, MRS Proceeding No. 196* (edited by M.J. Mayo, J. Wadsworth, and M. Kobayashi), p. 325, Materials Research Society, Pittsburgh, PA (1990).
32. R. Duclos, J. Crampon, and B. Amana, *Acta Metall.*, **70**, 877 (1987).
33. T.G. Nieh and J. Wadsworth, *Scr. Metall. Mater.*, **24**, 763 (1990).
34. W.J. Kim, J. Wolfenstine, and O.D. Sherby, *Acta Metall. Mater.*, **39**, 199 (1991).
35. S.E. Dougherty, T.G. Nieh, J. Wadsworth, and Y. Akimune, *J. Mater. Res.*, (1995). – in press
36. T.G. Nieh, D.L. Yaney, and J. Wadsworth, *Scripta Metall.*, **23**, 2007 (1989).
37. F. Wakai, H. Okamura, N. Kimura, and P.G.E. Descamps, *Proc. 1st Japan Int'l SAMPE Symp.* (edited by N. Igata, K. Kimpara, T. Kishi, E. Nakata, A. Okura, and T. Uryu), p. 267, Society for the Advancement of Materials and Process Engineering (1989).
38. L.A. Xue, *J. Mater. Sci. Lett.*, **10**, 1291 (1991).
39. S. Hanada, T. Sato, S. Watanabe, and O. Izumi, *J. Jpn Inst. Metals*, **45**, 1293 (1981).

40. V.K. Sikka, C.T. Liu, and E.A. Loria, *Processing of Structural Metals by Rapid Solidification* (edited by F.H. Froes and S.J. Savage), p. 417, Am. Soc. Metals, Metals Park, OH (1987).
41. M.S. Kim, S. Hanada, S. Wantanabe, and O. Izumi, *Mater. Trans. JIM*, **30**, 77 (1989).
42. A. Choudhury, A.K. Muhkerjee, and V.K. Sikka, *J. Mater. Sci.*, **25**, 3142 (1990).
43. T.G. Nieh and W.C. Oliver, *Scr. Metall.*, **23**, 851 (1989).
44. T. Takasugi, S. Rikukawa, and S. Hanada, *Acta Metall. Mater.*, **40**, 1895 (1992).
45. D. Lin, A. Shan, and D. Li, *Scr. Metall. Mater.*, **31**, 1455 (1994).
46. S.C. Cheng, J. Wolfenstine, and O.D. Sherby, *Metall. Trans.*, **23A**, 1509 (1992).
47. T. Tsujimoto, K. Hashimoto, and M. Nobuki, *Mater. Trans., JIM*, **33**, 989 (1992).
48. W.B. Lee, H.S. Yang, Y.-W. Kim, and A.K. Muhkerjee, *Scr. Metall. Mater.*, **29**, 1403 (1993).
49. A. Dutta and D. Banerjee, *Scr. Metall. Mater.*, **24**, 1319 (1990).
50. H.S. Yang, P. Jin, E. Dalder, and A.K. Muhkerjee, *Scr. Metall. Mater.*, **25**, 1223 (1991).
51. S.L. Stoner and A.K. Muhkerjee, *International Conference on Superplasticity in Advanced Materials (ICSAM-91)* (edited by S. Hori, M. Tokizane, and N. Furushiro), p. 323, The Japan Society for Research on Superplasticity (1991).
52. O.D. Sherby and J. Wadsworth, *Deformation, Processing and Structure* (edited by G. Krauss), p. 355, ASM, Metal Park, Ohio (1984).
53. J.K. Gregory, J.C. Gibeling, and W.D. Nix, *Metall. Trans.*, **16A**, 777 (1985).
54. T. Takasugi, S. Rikukawa, and S. Hanada, *Scr. Metall. Mater.*, **25**, 889 (1991).
55. N. Ridley, M.F. Islam, and J. Pilling, *Structural Intermetallics* (edited by R. Darolia, J.J. Lewandowski, C.T. Liu, P.L. Martin, D.B. Miracle, and M.V. Nathal), p. 63, TMS, Warrendale, PA (1993).
56. R.M. Imayev, O.A. Kaibyshev, and G.A. Salishchev, *Acta Metall. Mater.*, **40**, 581 (1992).
57. D. Vanderschueren, M. Nobuki, and M. Nakamura, *Scr. Metall. Mater.*, **28**, 605 (1993).
58. M. Tokizane, T. Fukami, and T. Inaba, *ISIJ Inter.*, **10**, (1991).
59. S.L. Kampe, J.D. Bryant, and L. Christodoulou, *Metall. Trans.*, **22A**, 447 (1991).
60. F. Wakai, *Brit. Ceram. Trans. J.*, **88**, 205 (1989).
61. X. Wu and I.W. Chen, *J. Am. Ceram. Soc.*, **73**, 746 (1990).
62. J.P. Wittenauer, T.G. Nieh, and J. Wadsworth, *J. Am. Ceram. Soc.*, **76**, 1665 (1993).
63. T.G. Nieh and J. Wadsworth, *J. Mater. Eng. Performance*, **3**, 496 (1994).
64. T.G. Nieh, LMSC-F070359, pp.7-301-7-321, Lockheed Missiles and Space Co. (1986).
65. T.G. Nieh and J. Wadsworth, *MRS Intl. Meeting on Advanced Materials Vol 7 (IUMRS-ICAM-93, Symp. E, Superplasticity)* (edited by M. Doyama, S. Somiya, and R.P.H. Chan), Pergamon Press, Netherland (1994). – in press
66. K. Watanabe, private communication, NGK Insulators, Ltd., Nangoya, Japan (1994).
67. D. Shih, private communication, McDonnell Douglas, St. Louis, MO (1994).
68. J.P. Wittenauer, C. Bassi, and B. Walser, *Scr. Metall.*, **23**, 1381 (1989).
69. Y. Nishiyama, T. Miyashita, S. Isobe, and T. Noda, *High Temperature Aluminides & Intermetallics* (edited by S.H. Whang, C.T. Liu, D.P. Pope, and J.O. Stiegler), p. 557, The Minerals, Metals, and Materials Society (1990).